

# MOLECULAR DYNAMICS SIMULATION OF HETEROGENEOUS NUCLEATION OF LIQUID DROPLET ON SOLID SURFACE

Tatsuto Kimura\* and Shigeo Maruyama\*\*

\*Department of Mechanical Engineering, The University of Tokyo  
7-3-1 Hongo, Bunkyo-ku, Tokyo 113-8656, Japan

\*\*Engineering Research Institute, The University of Tokyo  
2-11-16 Yayoi, Bunkyo-ku, Tokyo 113-8656, Japan

## ABSTRACT

The heterogeneous nucleation of liquid droplet on a solid surface was simulated with the molecular dynamics method. Argon vapor was represented by 5760 Lennard-Jones molecules and the solid surface was represented by one layer of 1020 harmonic molecules with the constant temperature heat bath model using the phantom molecules. The potential parameter between solid molecule and vapor molecule was changed to reproduce various surface wettabilities. After the equilibrium condition at 160 K was obtained, temperature of the solid surface was suddenly set to 100 K or 80 K by the phantom molecule method. The observed nucleation rate, critical nucleus size and free energy needed for cluster formation were not much different from the prediction of the classical heterogeneous nucleation theory in case of smaller cooling rate. The difference became considerable with the increase in cooling rate and with increase in surface wettability because of the spatial temperature distribution.

## 1. INTRODUCTION

The liquid droplet nucleation on a solid surface is very important phenomena from the viewpoint of the dropwise condensation theory, and is also very interesting related to the nanotechnology such as the quantum dot generation. We have simulated the equilibrium liquid droplet on the solid surface by the molecular dynamics method, and have clarified the relationship between potential parameter of molecules and macroscopic quantities such as contact angle [1]. In addition, we have carried out the molecular dynamics simulation on the bubble nucleation process on the solid surface [2]. In the meantime, direct molecular dynamics simulations of the homogeneous nucleation process were performed by Yasuoka et al. for the Lennard-Jones fluid [3] and water [4], and a large discrepancy from the classical nucleation theory was reported. Here, the heterogeneous nucleation of liquid droplet on solid surface was directly simulated by the molecular dynamics method and the nucleation rate was compared with the classical nucleation theory.

## 2. SIMULATION METHOD

As shown in Fig. 1, vapor argon consisted of 5760 molecules in contact with plane solid surface was prepared. The potential between argon molecules was represented by the well-known Lennard Jones (12-6) function as

$$\phi(r) = 4\epsilon \left\{ \left( \frac{\sigma}{r} \right)^{12} - \left( \frac{\sigma}{r} \right)^6 \right\} \quad (1)$$

where the length scale  $\sigma_{AR} = 3.40 \times 10^{-10}$  m, energy scale  $\epsilon_{AR} = 1.67 \times 10^{-21}$  J, and mass  $m_{AR} = 6.63 \times 10^{-26}$  kg. We used the potential cut-off at  $3.5\sigma_{AR}$  with the shift of the function for the

continuous decay [5].

$$\phi_{SF}(r) = 4\epsilon \left[ \left\{ \left( \frac{\sigma}{r} \right)^{12} - \left( \frac{\sigma}{r} \right)^6 \right\} + \left\{ 6 \left( \frac{\sigma}{r_c} \right)^{12} - 3 \left( \frac{\sigma}{r_c} \right)^6 \right\} \left( \frac{r}{r_c} \right)^2 - \left\{ 7 \left( \frac{\sigma}{r_c} \right)^{12} - 4 \left( \frac{\sigma}{r_c} \right)^6 \right\} \right] \quad (2)$$

The solid surface was represented by one layer of 4464 harmonic molecules in fcc (111) surface. Here, we set as: mass  $m_S = 3.24 \times 10^{-27}$  kg, distance of nearest neighbor molecules  $R_0 = 2.77 \times 10^{-10}$  m, and the spring constant  $k = 46.8$  N/m from the

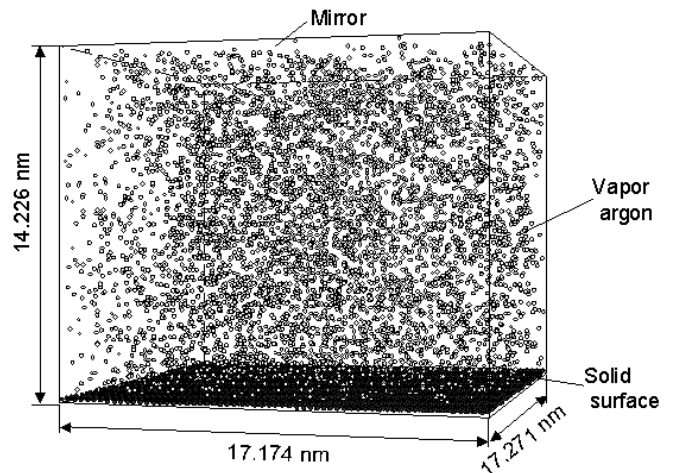


Figure 1 Simulation system.

Table 1 Calculation conditions.

Label	$\epsilon_{INT}$ [ $\times 10^{-21}$ J]	$\theta$ [deg]	$T_{wall}$ [K]	$T_{ave}$ [K]	$J_{sim}$ [ $\text{cm}^{-2} \text{s}^{-1}$ ]	$J_{th}$ [ $\text{cm}^{-2} \text{s}^{-1}$ ]	$J_{th}(\text{local})$ [ $\text{cm}^{-2} \text{s}^{-1}$ ]
E1	0.426	135.4	100	108	$6.52 \times 10^{20}$	$4.86 \times 10^{21}$	$4.50 \times 10^{21}$
E2	0.612	105.8	100	114	$3.45 \times 10^{21}$	$4.47 \times 10^{21}$	$1.45 \times 10^{22}$
E3	0.798	87.0	100	120	$5.76 \times 10^{21}$	$5.54 \times 10^{20}$	$7.01 \times 10^{22}$
E1-L	0.426	135.4	80	111	$3.96 \times 10^{21}$	$2.23 \times 10^{21}$	$7.62 \times 10^{21}$
E2-L	0.612	105.8	80	126	$1.41 \times 10^{22}$	( $10^{-134}$ )	$4.32 \times 10^{22}$
E3-L	0.798	87.0	80	129	$2.96 \times 10^{22}$	N-A	$1.44 \times 10^{23}$

physical properties of solid platinum crystal. We have controlled the temperature of the solid surface by arranging a layer of phantom molecules beneath the ‘real’ surface molecules. The phantom molecules modeled the infinitely wide bulk solid kept at a constant temperature  $T_{wall}$  with proper heat conduction characteristics [6, 7]. In practice, a solid molecule was connected with a phantom molecule with a spring of  $2k$  in vertical direction and springs of  $0.5k$  in two horizontal directions. Then, a phantom molecule was connected to the fixed frame with a spring of  $2k$  and a damper of  $\alpha = 5.184 \times 10^{-12}$  kg/s in vertical direction and springs of  $3.5k$  and dampers of  $\alpha$  in two horizontal directions. A phantom molecule was further excited by the random force in gaussian distribution with the standard deviation

$$\sigma_F = \sqrt{\frac{2\alpha k_B T}{\Delta t}} \quad (3)$$

where  $k_B$  is Boltzmann constant. This technique mimicked the constant temperature heat bath, which conducted heat from and to ‘real’ surface molecules as if a bulk solid was connected.

The potential between argon and solid molecule was also represented by the Lennard-Jones potential function. The length scale of the interaction potential  $\sigma_{INT}$  was kept constant as  $3.085 \times 10^{-10}$  m. In our previous study on the liquid droplet on the surface [1], we have found that the depth of the integrated effective surface potential

$$\epsilon_{SURF} = \frac{4\sqrt{3}\pi}{5} \frac{\epsilon_{INT}\sigma_{INT}^2}{R_0^2} \quad (4)$$

was directly related to the contact angle of the surface. Hence, we used various energy scale parameter  $\epsilon_{INT}$  as in Table 1 to change the wettability.

The classical momentum equation was integrated by the Verlet’s leap-frog method with the time step of 5 fs. As an initial condition, an argon fcc crystal was placed at the center of the calculation domain. We used the velocity-scaling temperature-control directly to argon molecules for initial 100 ps. Then, switching off the direct temperature control, the system was run for 500 ps with the temperature control only from the phantom molecules until the equilibrium argon vapor was achieved. After the equilibrium condition at 160 K was obtained, the set temperature of phantom  $T_{wall}$  was suddenly lowered to 100K or 80 K, and the system was cooled from the solid surface. The supersaturation ratio

$$S = \frac{\rho}{\rho_e} \quad (5)$$

was evaluated to be about 6 and 40 at this stage, respectively.

#### 4. RESULTS AND DISCUSSIONS

Variation of argon temperature and pressure in response to the wall temperature change for E2 in Table 1 are shown in top panel of Fig. 2. Here, we define the ‘cluster’ as a interconnecting group of molecules whose intermolecular distances are less than  $1.2\sigma_{AR}$ . Change in number of monomer and maximum cluster size are plotted in Fig. 2. In order to clarify the sensitivity to the threshold value of cluster definition, the following analyses were repeated for another threshold value  $1.5\sigma_{AR}$ . As a result, no substantial differences were observed. After 500 ps from the start of the calculation, solid surface was rapidly cooled by the temperature control of phantom molecules, and the temperature of argon gradually decreased afterward, then the formation and growth of clusters were recorded.

In Fig. 3, the snapshots of nucleation process for E2 are shown. Here, for clarity, only the clusters made of more than 5 molecules are shown. Initial small clusters appeared and disappeared randomly in space. Then larger clusters grew preferentially near the surface. Some of largest clusters near

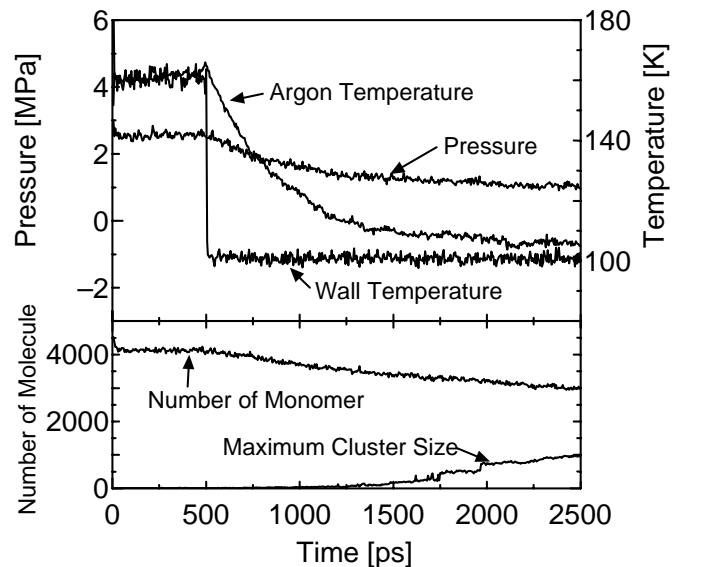


Figure 2 Variations of Pressure, temperature, number of monomer and maximum cluster size for E2.

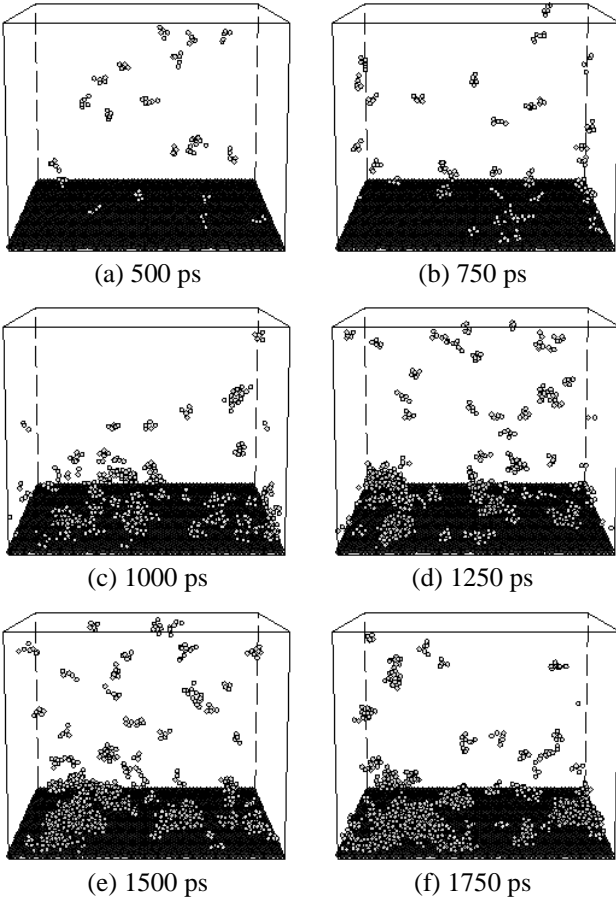


Figure 3 Snapshots of nucleation process for E2.

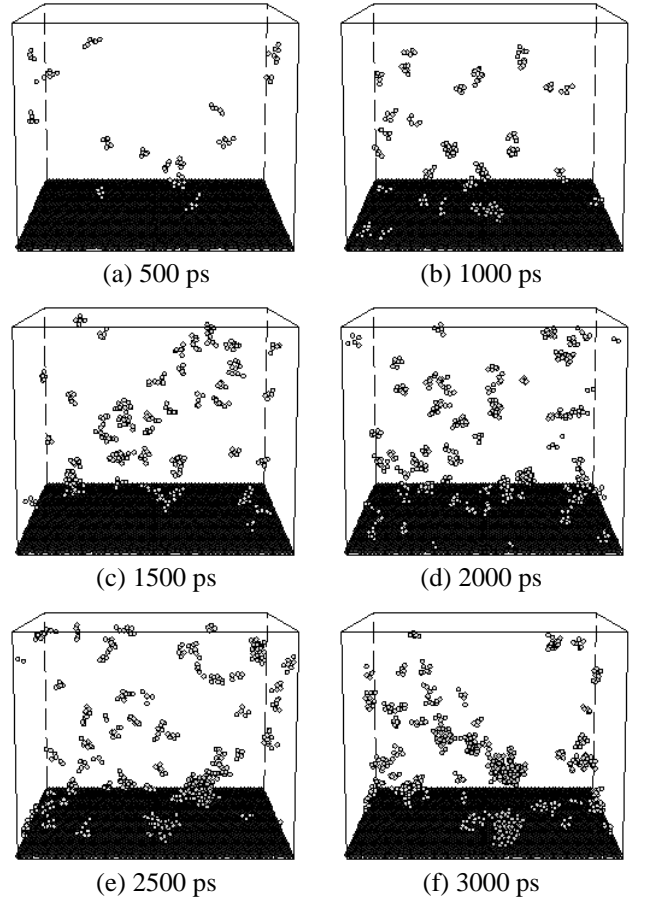


Figure 4 Snapshots of nucleation process for E1.

the surface continued to grow until the end of the simulation. On the other hand, for the less wettable condition E1 in Fig. 4, relatively large clusters grew without the help of surface, similar to homogeneous nucleation.

The cluster size distributions  $c(n)$  for several instances (short-time average) are shown in Fig. 5. Compared to the natural equilibrium distribution in Fig. 5 (a), constant amount of increase of distribution for the size range beyond  $n = 10$  can be conceived. The cluster size distribution in the range  $1 < n < 20$  seemed to keep the same structure after 1000 ps, it is also observed that, most of clusters beyond  $n > 10$  are principally on surface for this wettability E2. The spikes in the larger cluster size range are due to small number of clusters further grew from this quasi-equilibrium distribution in the range  $1 < n < 20$ .

The variations of the numbers of clusters larger than some thresholds are shown in Fig. 6 as in the same manner as the results of homogeneous nucleation by Yasuoka et al. [3]. Dashed lines were fitted to the linear part of each increasing curve. These lines are almost parallel for the thresholds of over 20 or 30 and it shows that the clusters exceeded this size keep to stably growing. It was proposed that the nucleation rate was estimated from the gradients of these lines [3]. Nucleation rate estimated from the average gradient of lines over 30, 40 and 50 becomes  $J_{sim} = 3.45 \times 10^{21} \text{ cm}^{-2} \text{ s}^{-1}$ .

On the other hand, in the classical nucleation theory, nucleation rate  $J_{th}$  of the heterogeneous nucleation on the smooth solid surface is expressed as follows.

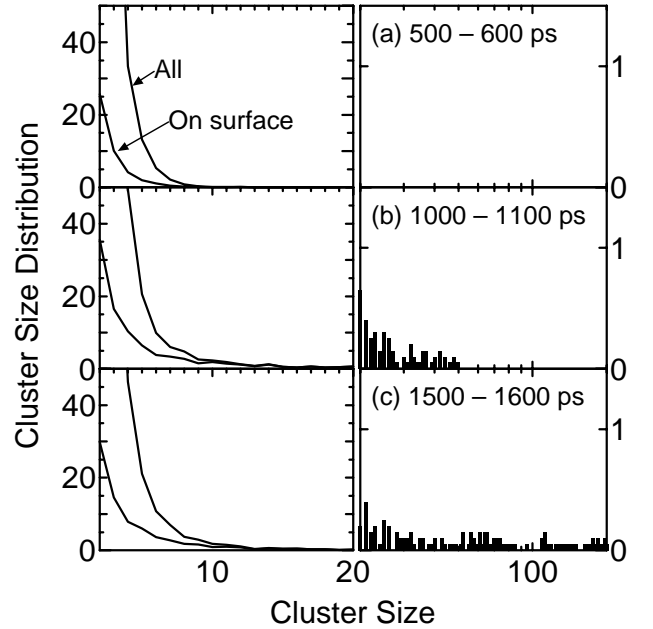


Figure 5 Clusters distribution for E2.

$$J_{th} = \rho^{\frac{2}{3}} \frac{\rho}{\rho_l} \frac{1 - \cos \theta}{2} \sqrt{\frac{2\gamma_{lv}}{\pi n f}} \exp\left(-\frac{\Delta G^*}{k_B T}\right) \quad (6)$$

$$f = \frac{1}{4} (2 - 3 \cos \theta + \cos^3 \theta)$$

$$\Delta G^* = \frac{16\pi r^3 f}{3(\rho_l k_B T \ln S)^2}$$

Using the average temperature  $T_{ave}$  and vapor density  $\rho$  in the period from 1000 ps to 1500 ps in which the number of clusters changed linearly in Fig. 6, the nucleation rate was calculated to be  $J_{th} = 4.47 \times 10^{21} \text{ cm}^{-2} \text{ s}^{-1}$ . Here, the values of the saturated vapor density  $\rho_e$  and liquid density  $\rho_l$  were calculated from the equation of state of Lennard-Jones fluid [8], and that of surface tension of liquid vapor interface  $\gamma_{lv}$  was employed from physical property of argon. Furthermore, the contact angle for each surface condition was estimated from our equilibrium simulation results [1]. The nucleation rate calculated from this simulation agreed with the classical nucleation theory very well in clear contrast to the 7 orders of difference for the homogeneous nucleation by Yasuoka et al. [3]. The critical cluster size in the classical nucleation theory is given in the following equation.

$$n^* = \frac{32\pi\gamma^3 f}{3\rho_l^2 (k_B T \ln S)^3} \quad (7)$$

It was calculated to be 16.5 for current condition. In this simulation, it was estimated to about 20 from the change of the gradients of the lines in Fig. 6, and the agreement was reasonable.

Cluster size distribution in the range smaller than the critical nucleus  $n^*$  is given in following equation in the classical theory.

$$c(n) = \rho^{\frac{2}{3}} \exp\left(-\frac{\Delta G}{k_B T}\right) \quad (8)$$

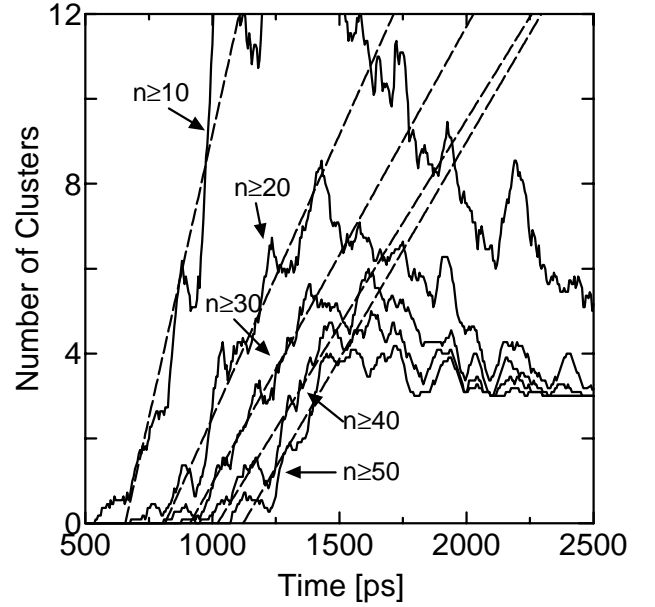


Figure 6 Variations of number of clusters larger than a threshold for E2.

The open circles in Fig. 7 shows the free energy needed for cluster formation  $\Delta G$  calculated using Eq. (8), from the average cluster distribution  $c(n)$  such as in Fig. 5 in the period in which clusters were stably forming. The solid line shows  $\Delta G$  given in the heterogeneous nucleation theory as follows.

$$\Delta G = \left(4\pi r^2 \gamma - \frac{4}{3}\pi r^3 \rho_l k_B T \ln S\right) f, \quad n = \frac{4}{3}\pi r^3 \rho_l f \quad (9)$$

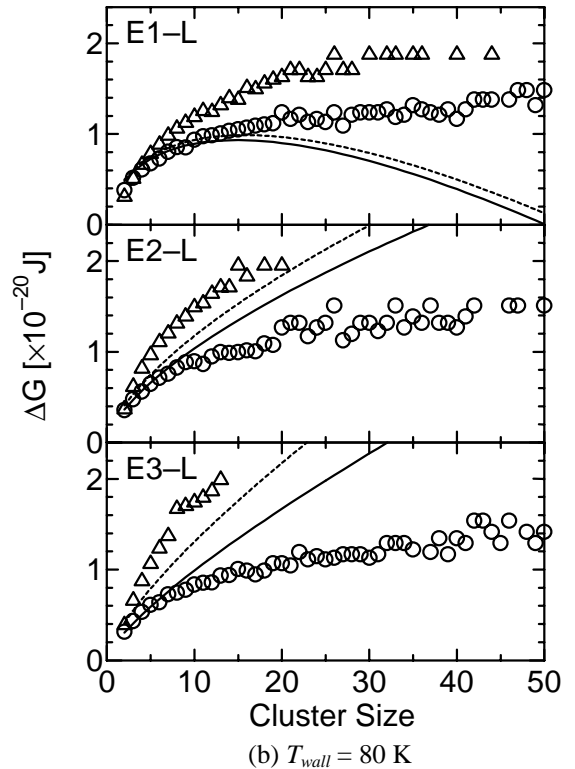
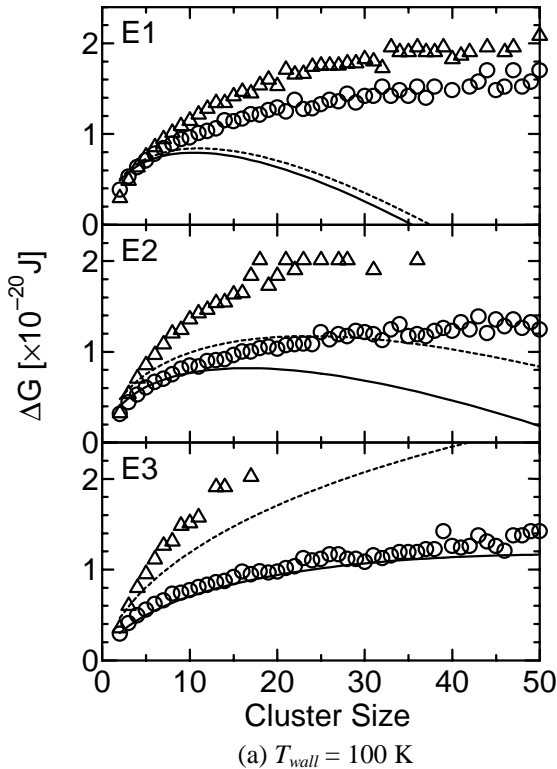


Figure 7 Cluster formation free energy.

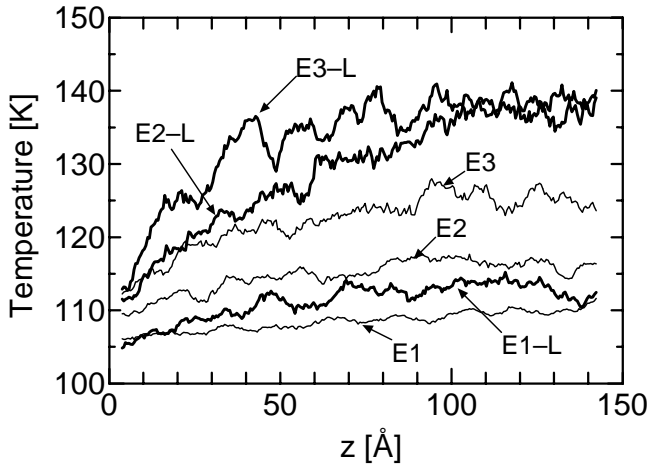


Figure 8 Temperature distribution during nucleation period.

Triangles and broken lines show  $\Delta G$  calculated from cluster distribution far from solid surface and from the classical homogeneous nucleation theory, respectively. Considering that Eq. (8) is effective only in the size range smaller than the critical nucleus where  $\Delta G$  is maximum in Eq. (9), it can be observed that  $\Delta G$  from heterogeneous nucleation theory and from cluster distribution in contacted with solid surface almost agree for the simulations in which the set temperature of the solid surface  $T_{wall}$  was higher (100 K). Furthermore,  $\Delta G$  from homogeneous nucleation theory and from cluster distribution far from the surface agreed well, though  $\Delta G$  of simulation was slightly larger. The similar comparison of free energy by Yasuoka et al. [3] showed the remarkable difference in the simulation results from the classical theory.

On the other hand, for the simulations in which  $T_{wall}$  was lower (80 K), the difference between simulation and theory increased in E2-L and E3-L, though it almost agreed in E1-L whose surface was less wettable. Actually the theoretical value of the nucleation rate  $J_{th}$  for E2-L was extremely small value and the classical theory predicts no nucleation for the case of E3-L with the supersaturation ratio of 0.87. The problem was in the steep vertical temperature distribution in our simulations. The vertical temperature distributions in the period in which clusters were stably forming were calculated as shown in Fig. 8. Considerably large temperature gradient has been given in E2-L and E3-L in which  $T_{wall}$  was lower and thermal boundary resistance [9] between liquid and solid surface was smaller than E1, E2 and E1-L. It can be understood that the difference from the classical nucleation theory tended to increase with the increase in the cooling rate because of the spatial temperature distribution.

Figure 9 shows density distribution and average temperature for E3-L. Since the cluster grew very near the surface in this case, the classical nucleation rate for the average temperature  $0 < z < 20$  was calculated. The classical nucleation rate for this local average temperature reasonably agreed with simulation result as shown in Table 1. The reason for the large discrepancy of Homogeneous results by Yasuoka et al. [3] is not clear yet. It can be speculated the cooling rate by collisions with buffer gas by Yasuoka et al. [3] may be too efficient.

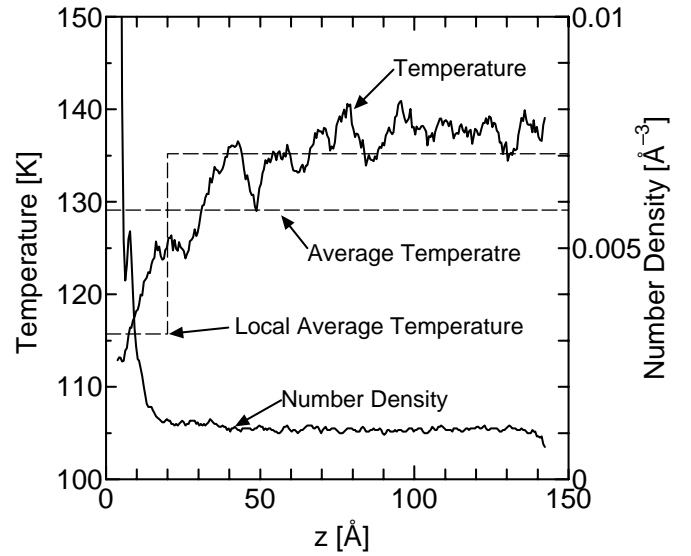


Figure 9 Density distribution and average temperature for E3-L.

## 5. CONCLUSION

We have successfully demonstrated the nucleation of 3-dimensional liquid droplet on the solid surface using the molecular dynamics method. Obtained nucleation rate, the critical nucleus size and free energy needed for cluster formation almost agreed with classical heterogeneous theory in case that cooling rate was smaller or the solid surface was less wettable. Because of the spatial temperature distribution, the difference became larger with the increase in cooling rate and surface wettability. However, with the definition of local average temperature, the simulation results were almost explained by the classical theory.

## 6. ACKNOWLEDGEMENT

Part of this work was supported by Grand-in-Aid for Scientific Research (B) (No. 12450082) from the Ministry of Education, Science, Sports and Culture, Japan.

## 7. NOMENCLATURE

- $c(n)$ : Number distribution function of clusters
- $f$ : Function in classical heterogeneous nucleation theory
- $J$ : Nucleation rate,  $\text{cm}^{-2}\text{s}^{-1}$
- $k$ : Spring constant, N/m
- $k_B$ : Boltzmann constant, J/K
- $m$ : Mass, kg
- $n$ : Cluster size
- $R_0$ : Distance of nearest neighbor molecules, m
- $r$ : Radius or distance of two molecules, m
- $r_c$ : Cutoff radius, m
- $S$ : Supersaturation ratio
- $T$ : Temperature, K
- $T_{wall}$ : Set temperature of phantom molecules, K

## Greek Symbols

- $\alpha$ : Damping factor, kg/s
- $\Delta G$ : Free energy needed for cluster formation, J

$\Delta t$ : Time step, s  
 $\varepsilon$ : Energy parameter of Lennard-Jones potential, J  
 $\varepsilon_{SURF}$ : Depth of integrated effective surface potential, J  
 $\phi$ : Potential function, J  
 $\phi_{SF}$ : Shifted Lennard-Jones potential function, J  
 $\gamma_v$ : Surface tension of liquid vapor interface, N/m  
 $\theta$ : Contact angle, rad  
 $\rho$ : Number density, m<sup>-3</sup>  
 $\sigma$ : Length parameter of Lennard-Jones potential, m  
 $\sigma_F$ : Standard deviation of exciting force, N

#### Subscripts and superscripts

AR: Argon  
 ave: Average over nucleation period  
 e: Saturated vapor  
 INT: Interaction between argon and solid molecules  
 l: Liquid  
 S: Solid molecule  
 sim: Simulation  
 th: Classical nucleation theory  
 \*: Critical nucleus

## 8. REFERENCES

1. S. Maruyama, T. Kurashige, S. Matsumoto, Y. Yamaguchi and T. Kimura, Liquid Droplet in Contact with a Solid Surface, *Microscale Thermophysical Engineering*, vol. 2, no. 1, pp. 49-62, 1998.
2. S. Maruyama and T. Kimura, A Molecular Dynamics Simulation of a Bubble Nucleation on Solid Surface, *International Journal of Heat & Technology*, vol. 18, no. 1, pp. 69-74, 2000.
3. K. Yasuoka and M. Matsumoto, Molecular Dynamics of Homogeneous Nucleation in the Vapor Phase. I. Lennard-Jones Fluid, *Journal of Chemical Physics*, vol. 109, no. 19, pp. 8451-8462, 1998.
4. K. Yasuoka and M. Matsumoto, Molecular Dynamics of Homogeneous Nucleation in the Vapor Phase. II. Water, *Journal of Chemical Physics*, vol. 109, no. 19, pp. 8463-8470, 1998.
5. S. D. Stoddard and J. Ford, Numerical Experiments on the Stochastic Behavior of a Lennard-Jones Gas System, *Physical Review A*, vol. 8, pp. 1504-1512, 1973.
6. J. C. Tully, Dynamics of Gas-Surface Interactions: 3D Generalized Langevin Model Applied to fcc and bcc Surfaces, *Journal of Chemical Physics*, vol. 73, no. 4, pp. 1975-1985, 1980.
7. J. Blömer and A. E. Beylich, Molecular Dynamics Simulation of Energy Accommodation of Internal and Translational Degrees of Freedom at Gas-Surface Interfaces, *Surface Science*, vol. 423, pp. 127-133, 1999.
8. J. J. Nicolas, K. E. Gubbins, W. B. Streett and D. J. Tildesley, Equation of State for the Lennard-Jones Fluid, *Molecular Physics*, vol. 37, no. 5, pp. 1429-1454, 1979.
9. S. Maruyama and T. Kimura, A Study on Thermal Resistance over a Solid-Liquid Interface by the Molecular Dynamics Method, *Thermal Science Engineering*, vol. 7, no. 1, pp. 63-68, 1999.